

Using of Geo-electrical and Geochemical Techniques to Investigate the Change in Ground Water Quality-South West El Khatbah City - Cairo-Alexandria Desert Road, Egypt

Ahmed N El Sayed^{1*}, Mostafa SM Barseem¹, Hosny M Ezz El Deen¹ and Hesham A Ezz El Din²

¹Geophysical Exploration Department, Desert Research Center, Egypt

²Hydrogeochemistry Department, Desert Research Center, Egypt

ABSTRACT

The agriculture investments on both sides of the Cairo-Alexandria desert road are suffering from the increase in salinity of the groundwater and effect on the sustainable development. The present study was applied to delineate the reasons and solutions for this problem. This study concentrates on the area lies at south-west El Khatbah city of Cairo-Alexandria desert way as a model. The investigated area is a part of the old alluvial plain which is characterized by a rolling surface sloping to the north and northeast. It contains sedimentary rocks belonging to Miocene, Pliocene, and the Quaternary times which are the most outcropping sediments. The water-bearing formation belongs to the Pleistocene, Lower Miocene (Moghra formation) and Oligocene aquifers. The last two aquifers are separated by the Oligocene basalt sheet. To achieve the aim of the study, a total of 12 Vertical Electrical Soundings (VES) in free wells and one 2D imaging with a roll along technique were carried out in the area of study. Also, the available data of 13 drilled wells were used that comprised lithological description, the thickness of the successive layers, water sample, and depth to water. The quantitative interpretation of the field curves revealed that the geoelectrical succession is formed of four main layers (A, B, C & D). The third geoelectrical layer (C) corresponding to saturated layer and divided into three zones (C1, C2 & C3) according to resistivity values. The first zone (C1) composed of clayey sand with resistivity values ranging from 15 to 26 Ohm.m and their thickness vary from 14 to 38 m. The second zone has relatively high resistivity value due to less clay content with sand. The resistivity value of this zone ranging from 21 and 40 Ohm.m and thickness varies from 20 to 40 m. The last geoelectrical zone does not extend all over the subsurface of the area due to faults with resistivity values ranging from 31 m to 54 Ohm.m. The high resistivity value is due to coarse sand but this zone end by clay content as well data. The thickness of this zones ranging from 16 to 50 m. The result of the roll along two-dimensional resistivity imaging profile refers to the heterogeneous character of the upper surface due to different degrees of clay contents that increase north western side of the investigated area. The three detected zones reflect three geoelectrical layers with different thickness due to the effect of two faults (F1 & F2) which throw northern trend detected that effect on the subsurface succession. The results of the analyzed samples were interpreted based on major ions and environmental stable isotopes determinations. Chemical analyses data revealed that most of the collected ground water samples from the Miocene aquifer are of fresh water type. Stable isotopic data ($\delta^{18}O$ and δD); showed that there is no contribution from rains to the groundwater. While mixing with the adjacent Pleistocene as well as the underlying Oligocene groundwater is confirmed.

Keywords: Vertical electrical soundings (VES), Multi-electrode gradient array, Roll-along technique, Groundwater, Geochemistry, Stable isotopes

INTRODUCTION

The West Nile Delta area is considered as a promising region to create new communities. The accessibility of the area,

its low relief, and availability of water made it easy to establish new settlements, land reclamation projects and other developmental projects. The recent projects include Wadi El Natrun and Wadi El Farigh, which have been established and subjected to future extensions. Limited water resources are the main problems to achieve the main target of constructing new settlements and land reclamation projects for sustainable development in the western Nile Delta. The available water resources include surface water (Rosetta branch and its irrigation channels) and relatively shallow groundwater that is mainly recharged from the surface water. Recently, surface Nile water is insufficient to meet all the Egyptian demand, especially in the future due to increasing of the population. Therefore, groundwater can partially help in providing some of the new projects by a significant amount of water. Groundwater is the main source for domestic, industrial and agriculture use in the western Nile Delta region [1]. The western Nile Delta contains four main groundwater aquifers. The water bearings formations belong to the Pleistocene, Pliocene, Miocene, and Oligocene. Many serious hydrogeological problems were concerning groundwater potentiality and degradation of its quality. Several factors play a significant role in the occurrence and supply of groundwater such as sedimentary succession, the geologic structure, lateral facies change and bad managements like over pump and random drilled wells. The present study considered as a trial to deal with these groundwater conditions that affect sustainable development.

The study area lies in the western Nile Delta region (Figure 1). It is at 70 km away from Cairo along the Cairo-Alexandria desert road. It is bounded by latitudes 30°12'40" to 30°14'37"N and longitudes 30°40'06" to 30°42'19". The present study aims to delineate the sedimentary succession and its vertical and lateral facies changes, the interface between miocene and oligocene aquifers formation, the impact of geological structures on the groundwater occurrence, the distribution of the basaltic sheet, hydrochemical characterizations of the groundwater, origin of the groundwater and evaluation of the groundwater suitability for different purposes. The geoelectrical resistivity and geochemical techniques deal with these subjects as a trail to contribute solving hydrogeological problems in the study area and its surroundings.

Many studies have been made to develop the western Nile Delta area. A series of studies was started in Wadi El Natrun area by Pavlov [2], Saad [3] and Shata [4]. Geoistrazivanja [5] reported the drilling results of test wells in the western desert fringes and four production wells along the Cairo-Alexandria Desert Road. La Moreaux [6] reported the hydrogeological condition in Wadi El Natrun area. A progressive report was carried out in by the staff of the Water Resources Department, Desert Institute, Egypt. El Shazly et al. [7] applied some of the remote sensing techniques on the western Nile Delta. Diab et al. [8] have studied the groundwater along Cairo-Alexandria Desert Road to the axis south of Wadi El Natrun and El Tahrir province. The recent studies including RIGW and IWACO indicate that the main recharge source for the groundwater in Wadi El Farigh and Wadi El Natrun was recent to old Nile water as well as some contributions from Western Desert Paleo-water [1,9-17]. The factors affecting the groundwater exploration were studied geoelectrical by Youssef [18], Barseem and El Sayed [19] used the geoelectrical method to study the factors affecting the groundwater quality in the area to the west of 117 km along the Cairo-Alexandria Desert road. Al-Abaseiry used the geoelectrical technique to solve the problem of salinization of the groundwater east of the Cairo-Alexandria desert way at 80 km. El Sheikh et al. [20] studied the impacts of the basalt on the occurrence and potentiality of groundwater southwest the Nile Delta area.

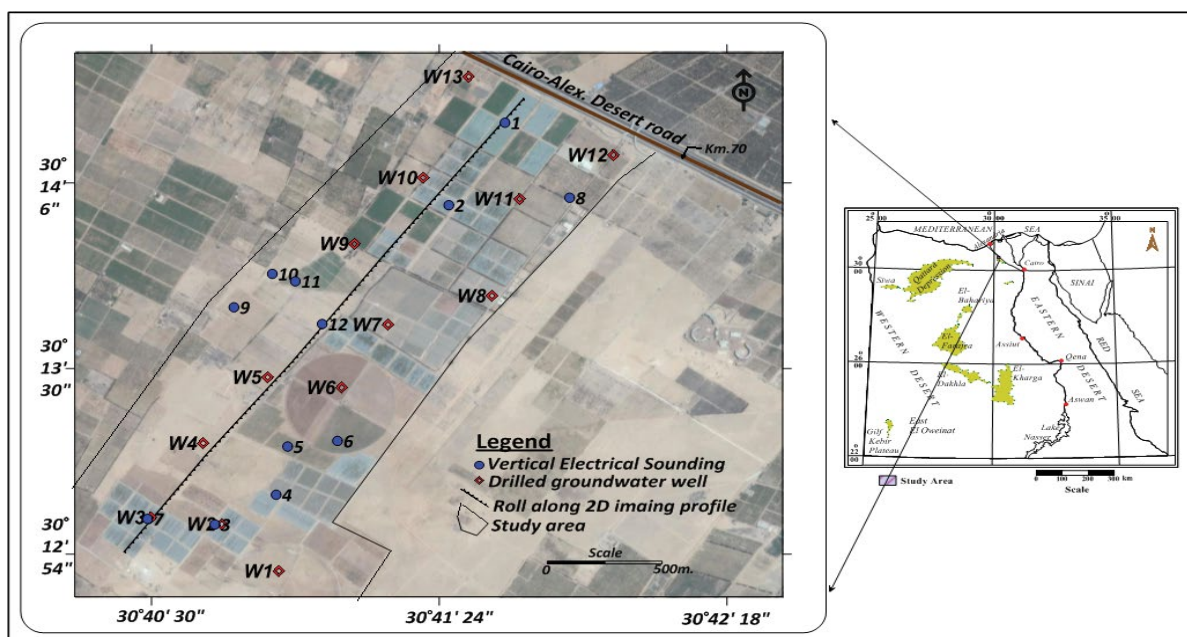


Figure 1: The location map of the study

GEOMORPHOLOGY, GEOLOGY, AND HYDROGEOLOGY

West of the Nile Delta area were studied by many authors aiming at delineating the geomorphological, geological and hydrological setting as Shata and El Fayoumy [21], Abdel Baki [22], Abd El Rahman [23].

Geomorphologic setting

The area west of the Nile Delta constitutes a portion of the great arid belt covering Egypt and is divided geomorphologically into four units [21] namely; the alluvial plains, the structural plains, the stable lands and the drifting sand. According to Abd El Baki [22], the alluvial plains are differentiated into two main units namely; young alluvial plains (recent floodplains) and old alluvial plains (gravelly terraces). The investigated area is a part of the old alluvial plain (Figure 2). This plain is characterized by a rolling surface sloping to the north and northeast, it is essentially underlain by dark brown gravel and coarse sand with fragments of fossil woods in the southern portions, while in the northern portion sandy deposits underlie it. Gravels form a portion of the Nile Delta terraces west of the Delta, assigned to Plio-Pleistocene and Early Pleistocene times [24]. The ground elevation of such terraces varies between +60 m near Wadi El Natrun and +20 m at the approach of the Delta.

The surface of the study area is dissected by shallow drainage lines, directed either to the Nile Delta basin or to Wadi El Natrun and Wadi El Farigh depressions. Such drainage lines acted as active creeks during the pluvial of the Pleistocene and the inter pluvials of the recent time. These creeks contributed to the supply of the sediments in the Nile Delta. Several shallow dendritic patterns dissect the old alluvial plains and the majority of them are mainly directed towards El Nubariya canal and Rosetta branch. Such drainage lines are filled by young sediments, which are mainly controlled by fracture systems and lithologic units. Small drainage lines (rills) are also known. These are associated with local catchments areas and are essentially directed to the inland desert depressions, where playa deposits are formed [25].

Geologic setting

The study area and its vicinities contain sedimentary rocks belonging to Miocene, Pliocene, and the Quaternary times which are the most outcropping sediments. It is dominated by Aeolian sand stretching all over the area in the form of sand sheets (Figure 3). These deposits are underlain by lagoonal deposits composed of gypsiferous sticky dark clay and sand. The lagoonal deposits overlie deltaic deposits consisting of medium quartz sand with variable amounts of gravels and clays. The base of the deltaic deposits is defined by Lower Pliocene pyretic clay or sandy clay overlies the Pliocene rocks (Tertiary) which are dominated by green clay [4]. The sedimentary rocks have a thickness of about 4500 m resting on the basement rocks [26]. The structural features that took place at the West Nile Delta area, are represented by folding, faulting, unconformities and basaltic intrusions.

Hydrogeologic setting

The investigated area and its vicinities characterized by an arid to a semi-arid climate with hot summer and mild rainy winter. The water-bearing formation in the southwestern part of the Nile Delta belongs to the Pleistocene, Lower

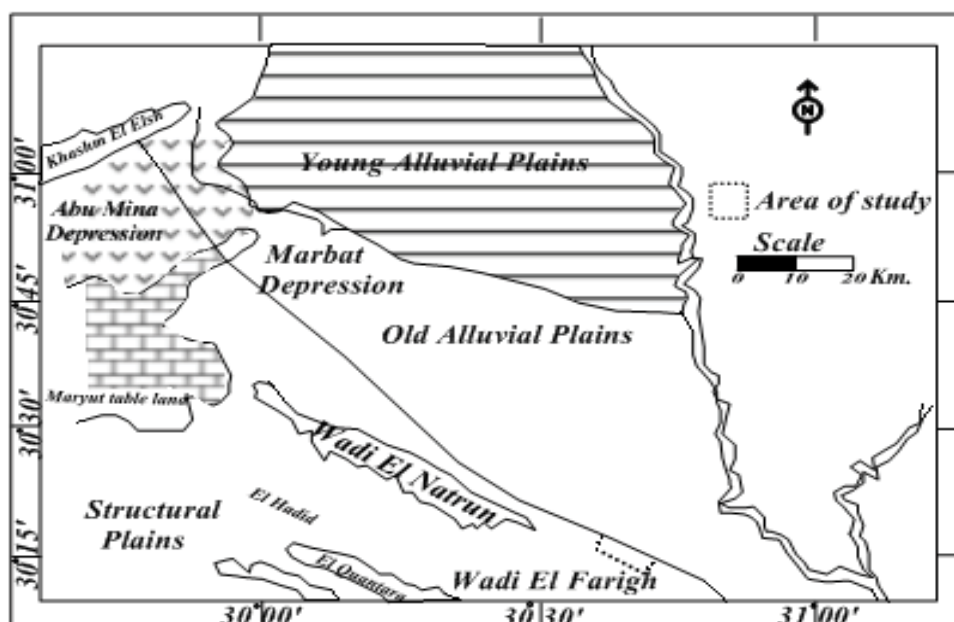


Figure 2: Geomorphology map of the study area (after Abd El Baki [22])

Miocene (Moghra formation) and Oligocene aquifers. The last two aquifers are separated by the Oligocene basalt sheet [27]. Emphasis will be given to the Miocene aquifer as it represents the main water-bearing formation in the area of study.

The Pleistocene aquifer

It is composed of successive layers of sand and gravel with some clay lenses. The thickness of this aquifer varies between 60 and 80 m near Wadi El Natrun and increases progressively eastwards. The Pleistocene aquifer is directly recharged from the main groundwater basin underlying the Nile Delta, the surface seepage from the cultivated lands as well as from the main irrigation canals. The groundwater of the Pleistocene aquifer varies in quality from fresh to brackish [22].

The Pliocene aquifer

It was considered as a multilayered aquifer system under confined and semi-confined conditions. It is composed of successive water-bearing layers (sand and sandstone) separated by impervious clayey layers and/or semi-permeable clayey sand layers. The aquifer is structurally controlled and hydraulically connected with the Pleistocene aquifer in Wadi El Natrun and Sadat city areas. Nile water and pale-water of deep aquifers, as well as the recent rainfall, were considered the main recharge sources to the aquifer [28-30].

The Miocene-Oligocene aquifer

It is essentially built of sand and sandstone with clay intercalation of fluvial and fluvio-marine origin, overlying the Oligocene basaltic sheets. The aquifer is hydraulically connected with the Oligocene and delta aquifers. Groundwater exists under unconfined to confined conditions [17]. The saturated thickness is controlled by the structural conditions. The Oligocene reservoir is a confined aquifer due to the presence of the basaltic sheet. The recharge of this aquifer may be due to the hydraulic connection with the overlying fractured Miocene aquifer.

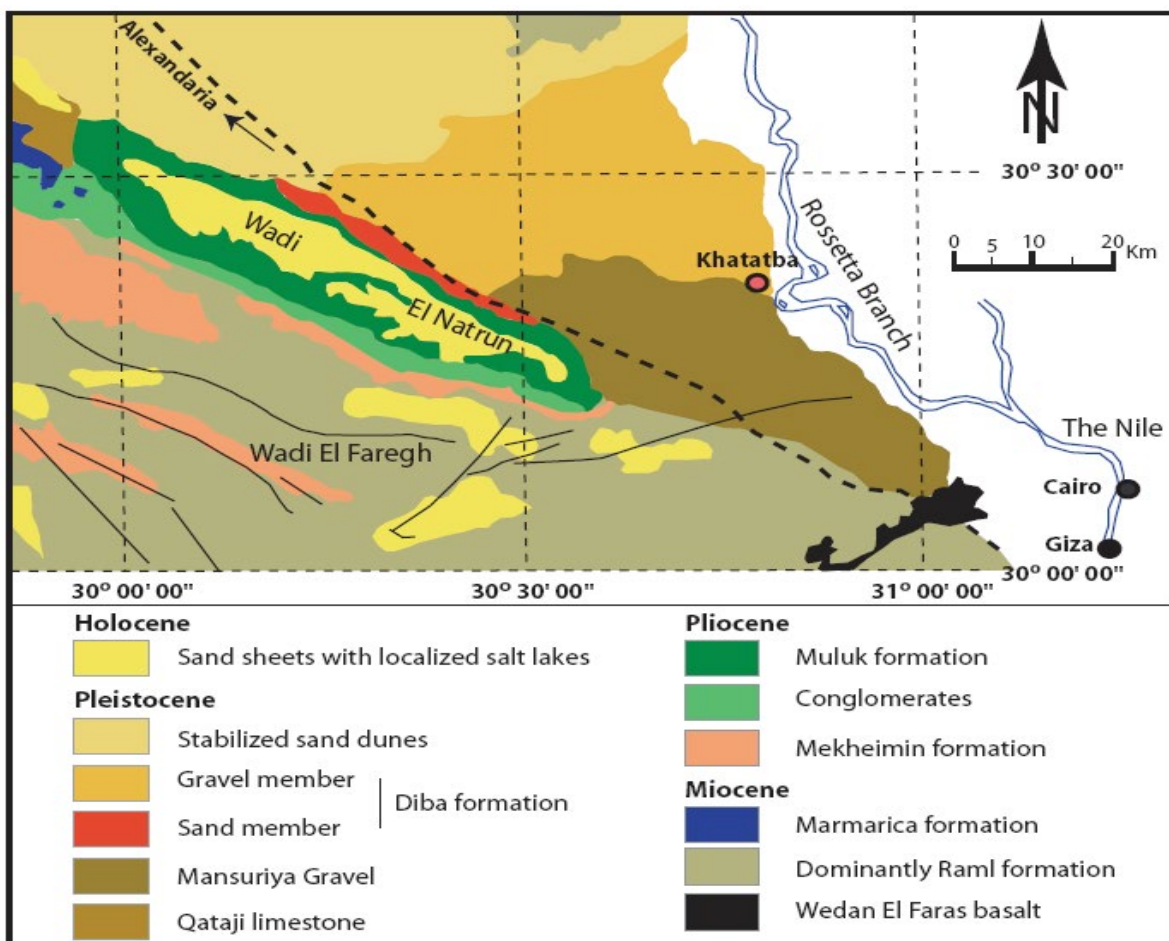


Figure 3: Regional geologic map of the study area (after CONOCO, 1987)

METHODOLOGY ANF FIELD MEASUREMENTS

The geophysical survey is a suitable technique for groundwater exploration, evaluation, and delineation the impact of the subsurface structures with the low cost. This survey can be further used in choosing the suitable sites for productive water-wells and their design without risk. To achieve the aim of the study, total of 12 Vertical Electrical Soundings (VES) in free wells and one 2D imaging with a roll along technique were carried out in the area of study. Also, the available data of 13 drilled wells were used that comprised lithological description, the thickness of the successive layers, water sample, and depth to water.

The Schlumberger electrode configuration was used in the VES measurements with a maximum current electrode separation (AB) 3000 m. This electrode separation was found to be sufficient to reach a reasonable depth range that fulfills the aim of the study. Two of these soundings were conducted beside a drilled well in order to parameterize and calibrate the geoelectrical interpretation. An arbitrary initial model has been constructed in view of the overall shape of the sounding curves and ties to some deep drilled wells. The RESIST computer program and (IP1 Win v.2.1, 2003) were applied for the quantitative interpretation of the geoelectrical sounding curves. It is interactive, graphically oriented, forward and inverses modeling program for interpreting the resistivity curves in terms of a layered earth model.

The 2D resistivity image obtained supply information which complements the one obtained with the more traditional Vertical Electrical Sounding (VES) technique. In the present study, 2D resistivity imaging carried with multi-electrode resistivity technique along one line reach in their length to about 3 km with Wenner arrays. The multi-electrode resistivity technique consists in using a multicore cable with as many conductors (72) as electrodes plugged into the ground at a fixed spacing every 20 m. After completing the sequence of measurements by the software automatically checks the electrode contact and scans through a predefined measurement protocol. Extension of the line is achieved through a roll-along technique, in which part of the layout is shifted by a quarter of the total layout length and new measurements are added (Figure 4). The interpretation of the 2D resistivity data has been carried out using the computer program RES2DINV, ver. 3.4 written by Dahlin and Loke [31]. The “Syscal Junior” resistivity meter is used for acquiring the geoelectrical measurements with high accuracy at different electrode spacing. The topographic survey is carried out to determine each electrode along different 2D imaging profiles by using the GPS apparatus (Trimble type) contacted with nine satellites.

The chemical characteristics of water are the titrimetric determination of carbonates (CO_3) and bicarbonates (HCO_3). While the other major constituents such as chloride (Cl), sulphate (SO_4), sodium (Na), potassium (K), calcium (Ca) and magnesium (Mg) ions were determined instrumentally by using ion chromatography (ICS-3000 Reagent-Free IC System). Environmental stable isotopes contents (O^{18} and Deutrium) of the collected water sample were determined according to the standard methods in the Isotope Geochemistry lab in the Department of Geosciences at Western Michigan University, Kalamazoo, Michigan, USA. The results were reported in delta per mile (‰) notation for O^{18} and deuterium (D).

RESULTS AND DISCUSSION

The integration between interpreted measured geoelectrical data and the chemical analysis of water samples was used to fulfill the objective of this study. The discussion of the obtained results as follows:

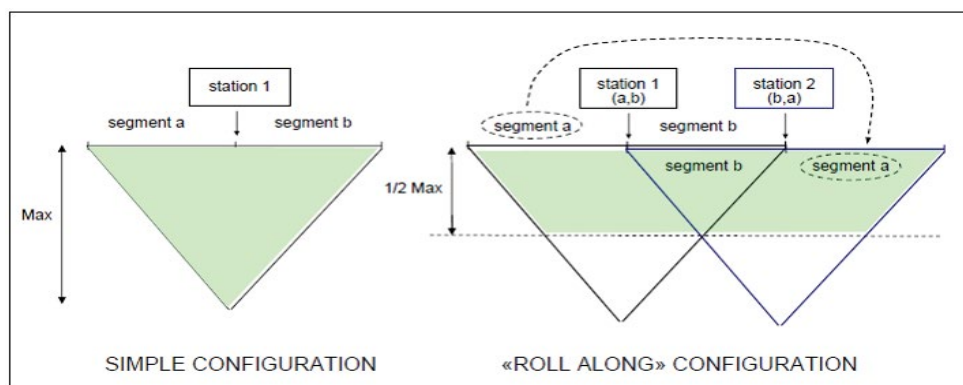


Figure 4: Depth of penetration in multi-electrode resistivity measurements (simple configuration (on left); roll along configuration (on right))

Interpretation of the geoelectrical data

The geoelectrical resistivity survey in the study area has been conducted by applying the conventional (1D and 2D roll along) techniques. The Vertical Electrical Sounding (1D) survey has been adopted with the purpose of determining the vertical and horizontal distribution of the sedimentary succession, the thickness of the water-bearing layers and detecting the subsurface geologic structures to clarify their impact on the groundwater occurrence. The two-dimensional electrical imaging (2D) scans the distribution of the electrical properties of the subsurface layers in the continuous image. A details result of these geoelectrical methods summarize as follows:

The vertical electrical sounding

The field data of the soundings have been interpreted qualitatively and quantitatively to delineate the subsurface sequence geologic setting in the area of study as the following:

Qualitative interpretation

The qualitative interpretation includes a comparison of the relative changes in the apparent resistivity and thicknesses of the different layers detected on the sounding curves (Figure 5). It gives information about the number of layers, their continuity throughout the area or in a certain direction and reflects the degree of homogeneity or heterogeneity of the individual layer. The field curves can be divided into two groups according to the end of all curves that reflect the common feature whereas the apparent resistivity is similar and the thicknesses (or depths) of the layers are different. This behavior can be observed when comparing the AB/2 values. So, some curves show H-type curve as reach to the basalt sheet of high resistivity values. These kinds of curve found on the southwestern side of the study area and revealed the basalt sheet near to the surface. The changes in the upper surface of basalt sheet due to faults. Other field curves end by K-type reflects the far away basalt sheet from surface especially on the northeastern side of the study area. On the first logarithmic cycle of all the field curves (i.e., at AB/2=1 to 10 m) show different trends and shapes so that a reasonable correlation is difficult to be conducted. However, they indicate and reflect heterogeneity characterizing the surface and near-surface variations (Figure 6). According to the geological evidence of the study area, the subsurface succession is characterized by a consisting of alternating layers of sand and clay that found as lenses.

Quantitative interpretation

The quantitative interpretation has been done to get a multiple layer model of true resistivity and thickness. The true resistivity values are related to lithology according to the geologic information of nearby wells. Figure 6 shows the interpretation of the modeled resistivity sounding VES No. 3 besides well No. 2. The general geologic setting and relevant information (structural elements) are visualized and described in view of a number of generated geoelectrical crossing in different directions. The quantitative interpretation of the field curves revealed that the geoelectrical succession is formed of four main layers (A, B, C & D) (Table 1) and the location of the geoelectrical cross sections are shown in Figure 7.

The (2D) imaging with roll along configuration

The interpretation of the 2D roll along imaging profile (Figures 7-12) shows three zones according to variation in resistivity values. The first zone shows resistivity ranging from (3-6 Ohm.m) corresponding to deposits of fine sand and clay. The second zone shows resistivity ranging from (24-91 Ohm.m) corresponding to deposits of saturated coarse sand and fractured basalt. The final zone shows high resistivity values

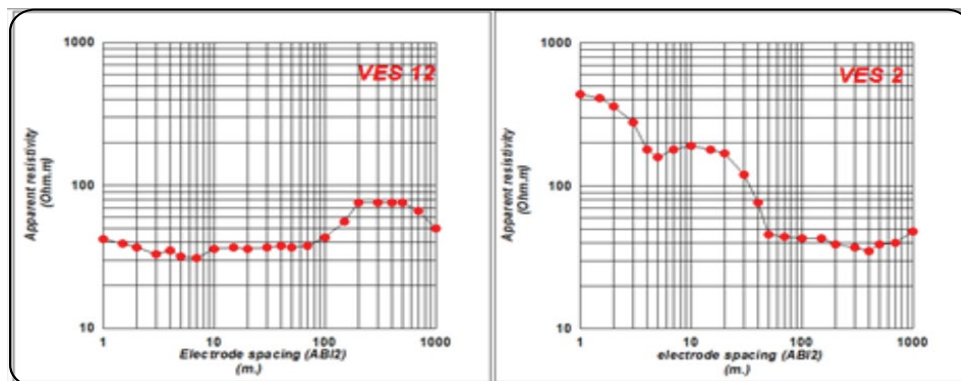


Figure 5: Examples of the resistivity sounding curves in the study area

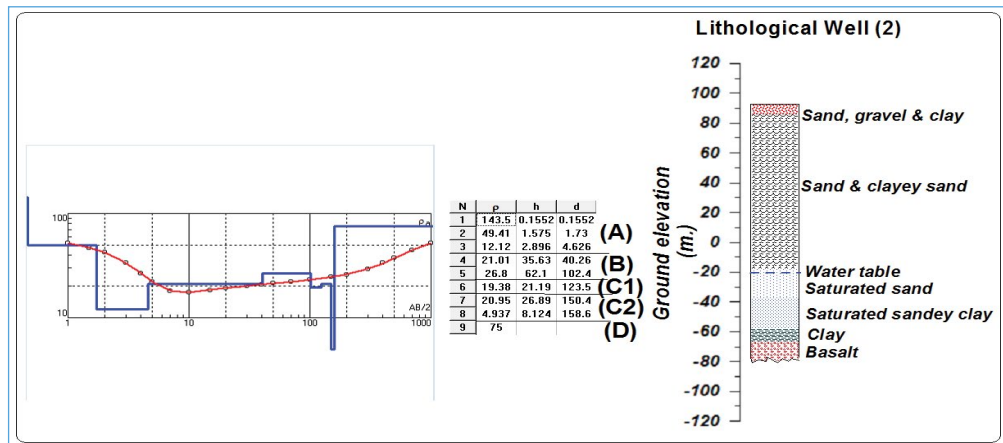


Figure 6: The interpretation of VES No. 3 beside well no. 2

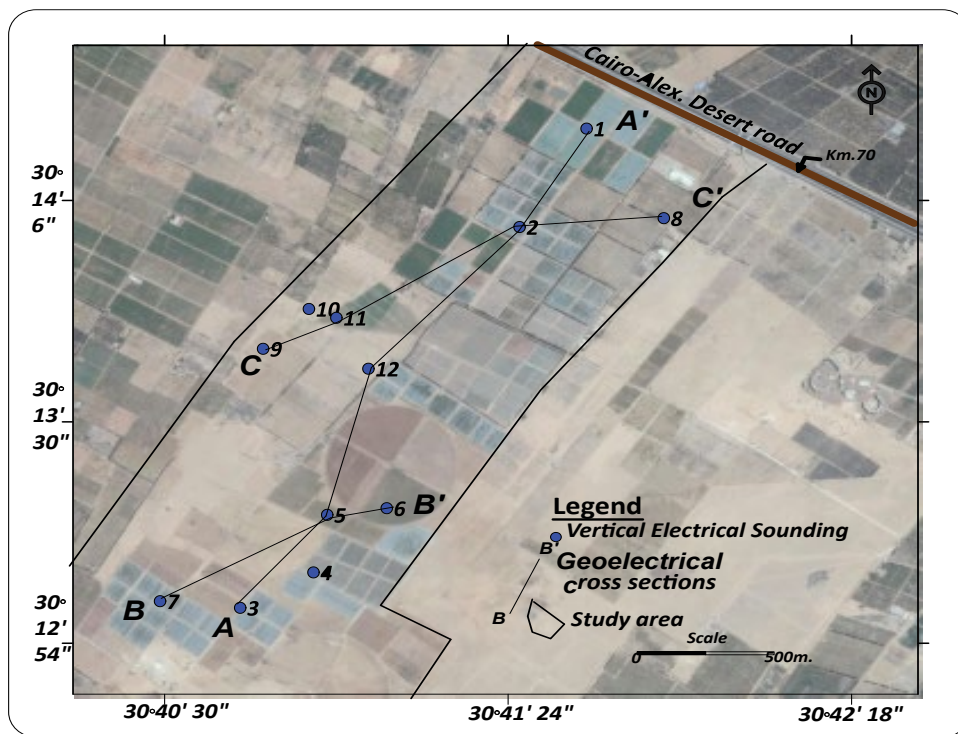


Figure 7: Location of the geoelectrical cross sections in the study area

greater than 179 Ohm.m corresponding to basalt sheet and compact of sand. These three zones reflect three geoelectrical layers with different thickness and two faults (F1 & F2) detected that affect the subsurface succession. The first geoelectrical layer as shown in the image of 2D roll along imaging profile has a wide variety from resistivity due to different lithological sediments with a thickness not exceeding 10 m. The second geoelectrical layer has thickness reach in some places to 80 m especially the north eastern side of the study area. This geoelectrical layer acts as a dry layer. According to surface geological and well logging data, the final geoelectrical layer act as saturated water bearing formation with thickness ranges from 60 and 110 m. This variation in thickness is mainly due to the effect of faults. The results obtained from 2D roll along imaging are compatible with the result of VES and well logging data.

Interpretation of the hydrochemical data

The entire database consists of chemical and isotopic analyses of 13 groundwater samples (Figure 13). The hydrochemical variables (consisting of major ions and isotope data) in the compiled database, were used in our evaluation. Hydrochemistry along with environmental isotopes (O18, D) studies was carried out to ascertain or deny the interrelationship between the different adjacent aquifers, especially Oligocene and Miocene in the study area.

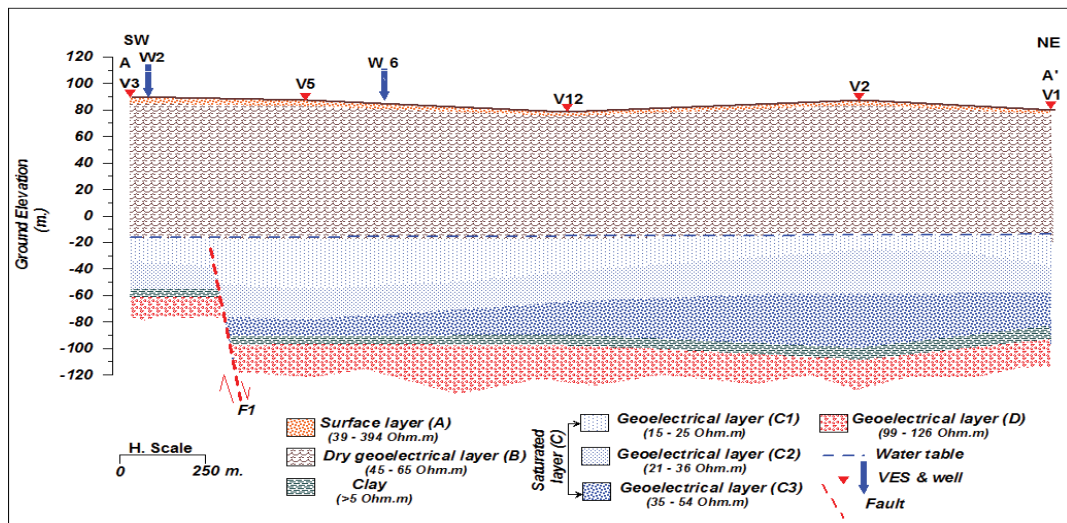


Figure 8: Geoelectrical cross section AA'

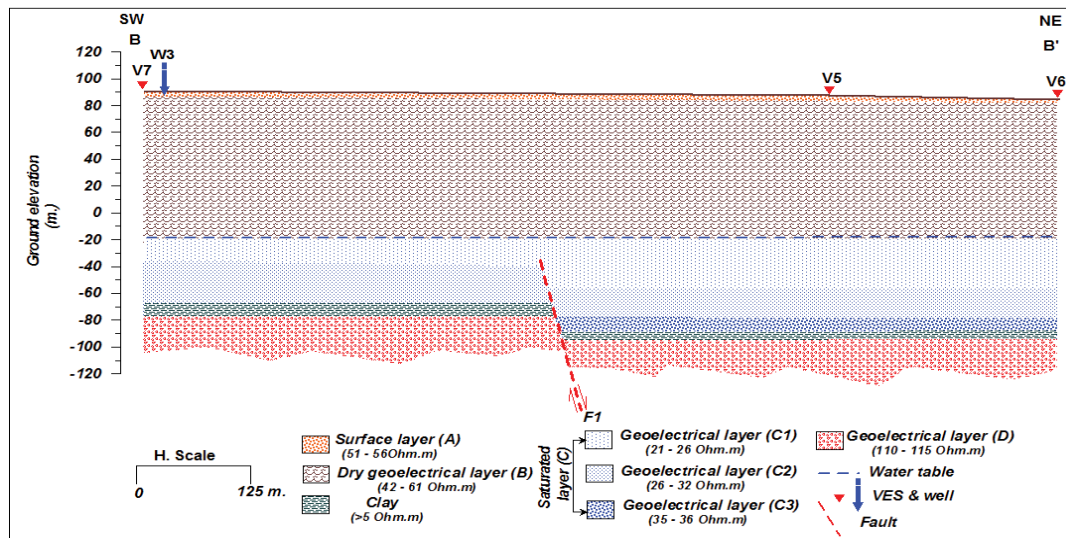


Figure 9: Geoelectrical cross section BB'

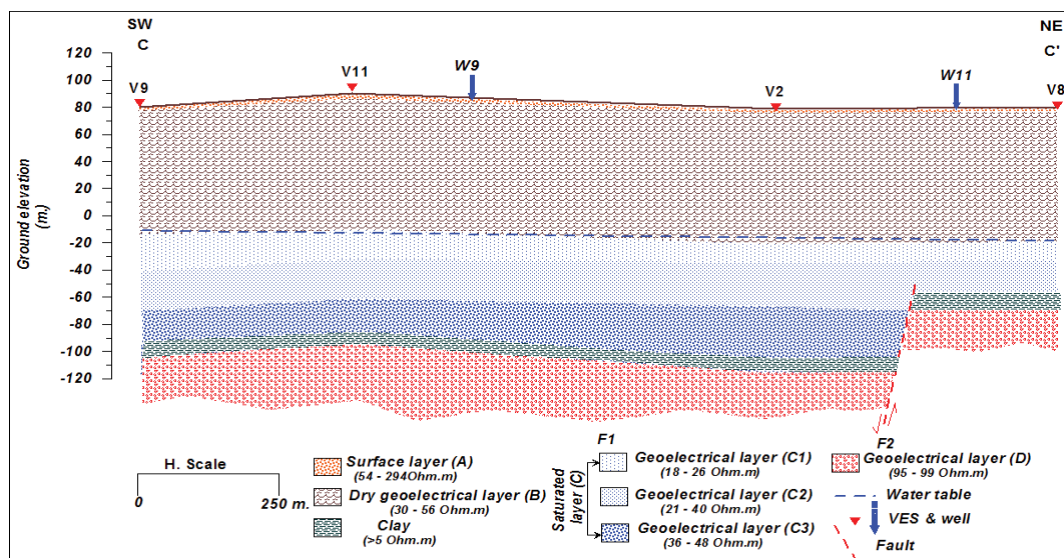


Figure 10: Geoelectrical cross section CC'

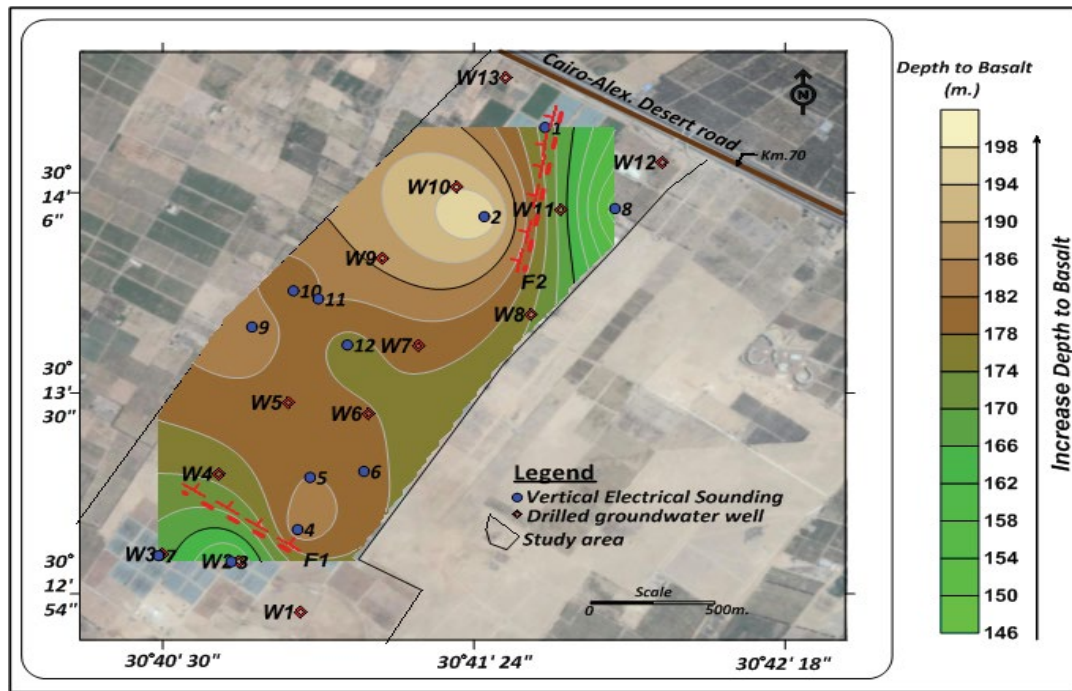


Figure 11: Structural contour map of the variation in depth to basalt from the ground elevation

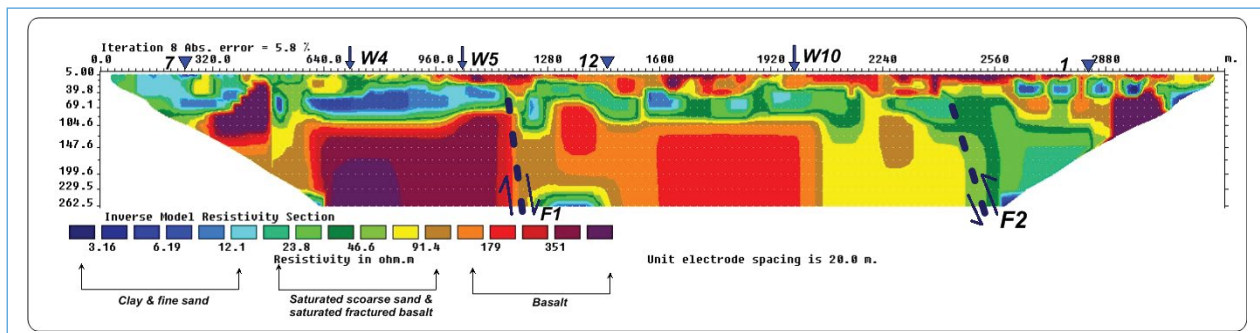


Figure 12: Inversion result of 2-D roll along imaging profile in the study area

ID	Name	Water type	EC	pH	TDS	Ca	Mg	Na	K	Cations	CO ₂	HCO ₃	SO ₄	Cl	Anions	D	O ¹⁸
W1	Pivot2	Na-Ca-Mg-HCO ₃	505	7.62	272	ppm	24.27	14.22	55.03	4.95	3.15	190.56	24.73	46.56	5.19	3.57	-0.33
						epm	1.21	1.17	2.39	0.13	4.90	0.10	3.25	0.52	1.31		
						%	24.71	23.86	48.84	2.58	100.00	2.02	62.72	9.95	25.31	100.00	
W2	Dokhan	Na-Mg-HCO ₃ -Cl	650	7.52	351	ppm	18.36	15.51	85.75	6.11	15.75	188.35	31.32	82.89	6.61	1.88	-0.55
						epm	0.92	1.01	3.75	0.16	6.11	0.52	3.10	0.65	2.34		
						%	14.99	21.41	51.04	2.56	100.00	7.94	46.84	9.96	35.36	100.00	
W5	Sakan2	Na-Ca-Mg-C-HCO ₃	1200	7.20	659	ppm	58.96	28.67	136.78	11.09	6.30	198.56	94.06	224.55	11.76	-0.39	-0.72
						epm	2.92	2.96	5.95	0.28	11.51	0.21	3.25	1.96	6.33		
						%	25.38	20.48	51.68	2.46	100.00	1.79	27.68	16.66	53.87	100.00	
W4	Tabba	Na-Ca-Mg-Cl	300	8.20	220	ppm	22.66	14.27	39.66	5.26	12.60	156.92	18.27	29.27	4.20	4.49	-0.26
						epm	1.13	1.17	1.73	0.13	4.16	0.42	2.57	0.38	0.83		
						%	27.15	28.18	41.43	3.23	100.00	10.00	61.27	9.06	15.66	100.00	
W5	Vārsha	Na-Ca-Mg-HCO ₃	1180	7.45	666	ppm	41.11	26.56	149.32	5.49	6.30	185.75	146.63	197.30	11.37	4.05	-0.30
						epm	2.05	2.18	6.50	0.14	10.87	0.21	3.04	3.05	5.56		
						%	18.87	20.09	59.75	1.29	100.00	1.77	25.64	25.72	46.86	100.00	
W6	Pivot1	Na-Mg-Ca-HCO ₃	460	6.91	235	ppm	18.89	14.51	45.01	5.12	9.45	195.35	19.38	24.10	4.60	3.94	-0.32
						epm	0.94	1.23	1.96	0.13	4.26	0.51	3.20	0.40	0.65		
						%	22.14	28.90	45.39	3.07	100.00	6.95	69.61	8.77	14.77	100.00	
W7	Kaharaba	Na-Mg-Ca-HCO ₃	455	7.88	226	ppm	18.99	13.20	47.45	3.34	12.60	172.94	18.60	24.41	4.33	4.47	-0.47
						epm	0.95	1.09	3.06	0.10	4.20	0.42	2.83	0.59	0.69		
						%	22.59	25.88	49.19	2.34	100.00	9.70	65.46	8.94	15.90	100.00	
W8	Sakan1	Na-Ca-Mg-C-HCO ₃	910	7.42	476	ppm	36.82	25.54	92.88	5.33	6.30	185.75	55.29	161.08	9.95	4.05	-0.51
						epm	1.82	2.10	4.04	0.14	8.10	0.21	3.04	1.15	4.54		
						%	22.50	25.94	49.88	1.68	100.00	2.35	34.02	12.87	50.76	100.00	
W9	Shaaban	Na-Cl-SO ₄	1180	7.60	1067	ppm	62.37	22.07	294.31	6.72	3.15	185.75	253.34	351.84	18.35	5.02	0.12
						epm	3.11	1.81	12.90	0.17	17.90	0.10	3.04	5.27	9.92		
						%	17.38	10.14	71.52	0.96	100.00	0.57	16.59	28.75	54.08	100.00	
W10	Basal	Na-Ca-Mg-C-HCO ₃	1175	7.22	646	ppm	78.56	27.20	119.85	12.95	3.15	140.91	119.03	215.32	10.96	4.52	-0.41
						epm	3.91	2.24	5.21	0.35	11.63	0.16	2.51	2.48	6.87		
						%	33.45	19.12	44.59	2.35	100.00	0.96	21.06	22.60	55.38	100.00	
W11	Mawaleh	Na-Ca-Mg-Cl	1465	7.66	785	ppm	82.94	46.77	120.58	6.42	9.45	160.13	89.95	348.07	14.61	3.30	-0.49
						epm	4.14	3.85	5.24	0.17	13.40	0.51	2.62	1.85	8.82		
						%	30.89	28.71	39.14	1.26	100.00	2.16	17.97	12.68	67.20	100.00	
W12	Mogamaa	Na-Ca-Mg-Cl	4500	7.70	2578	ppm	259.46	110.91	471.41	9.86	6.30	147.32	307.37	1338.56	46.77	3.98	-0.02
						epm	12.95	9.12	20.51	0.25	42.83	0.21	2.41	6.40	37.75		
						%	30.23	21.30	47.88	0.59	100.00	0.45	5.16	13.68	80.71	100.00	
W13	Masged	Na-Ca-Mg-HCO ₃	446	7.90	252	ppm	30.69	12.72	47.11	4.02	3.15	172.94	27.97	39.64	4.64	5.54	0.25
						epm	1.53	1.05	2.05	0.10	4.73	0.10	2.83	0.58	1.12		
						%	32.38	22.12	43.32	2.17	100.00	2.26	61.09	12.55	24.09	100.00	

Figure 13: The analyzed hydrochemical and isotopic items of groundwater samples

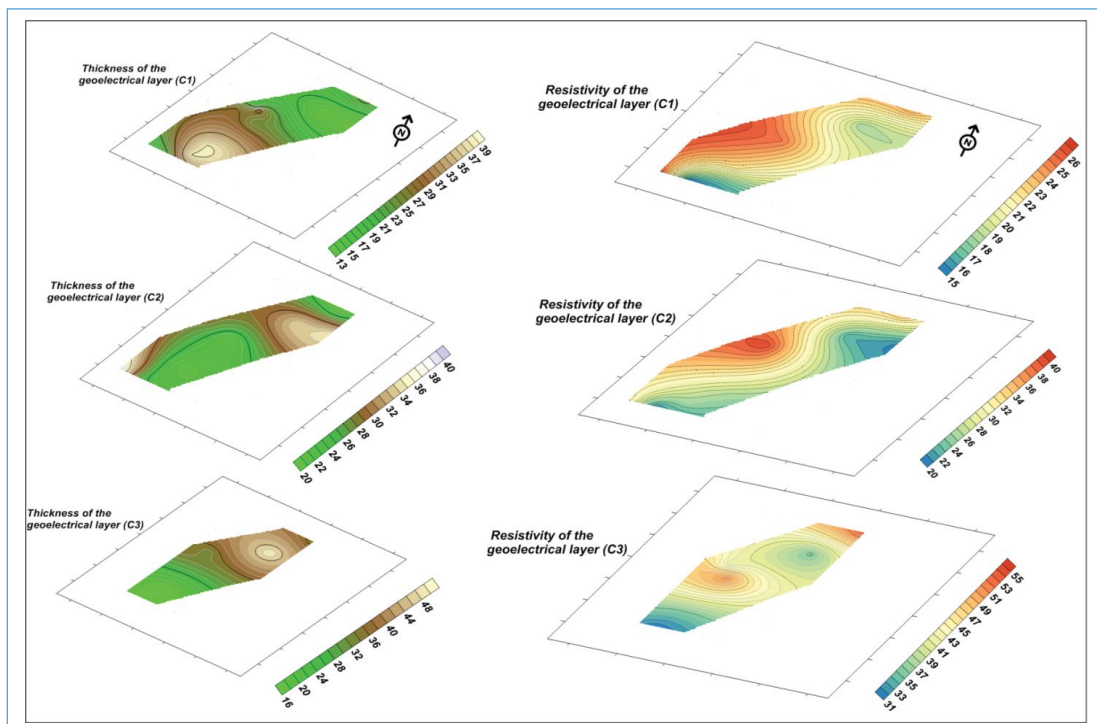


Figure 14: Contour maps of resistivity and thickness of the saturated layer (C)

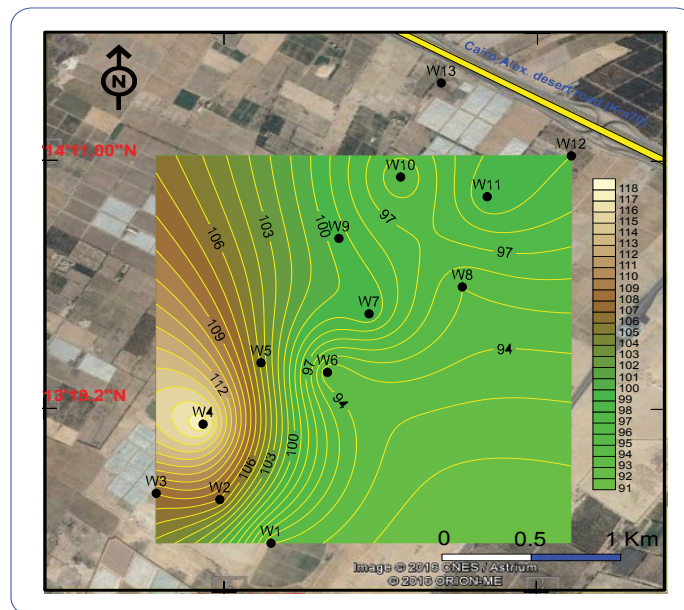


Figure 15: Groundwater flow direction

The nuclear techniques using the environmental stable isotopes $^{18}\text{O}/^{16}\text{O}$ and $^2\text{H}/^1\text{H}$ and radioactive isotope ^3H in groundwater, in its relation with surface water, provide adequate approach from which valuable pieces of information concerning water origin, flow and mixing could be obtained. The available major solute and environmental stable isotopic data were compiled for this study in order to create a comprehensive database, for the classification of waters into hydrochemical facies representing “water types”.

ASSESSMENT OF GROUNDWATER AQUIFER

The hydrologic data of the drilled wells throughout the study area indicate that the groundwater exists in Miocene and Oligocene aquifers. Some factors affected on the groundwater potentialities quantitatively and qualitatively. These

factors caused a series of hydrogeological problems that retard the prospective sustainable development in the study area and its vicinities. The details of the groundwater condition can be delineated by integration of the geoelectrical and geochemical results as follow:

The saturated geoelectrical layers (C)

The interpretation of geoelectrical sounding in the study area revealed that the saturated geoelectrical layer (C) is divided into three zones according to resistivity values (C1, C2 & C3). Figure 14 shows contour maps for both iso-resistivity and isopach of these saturated units (C1, C2 & C3). The first zone (C1) has relatively low resistivity values than other units (C1, C2) that range from 15-26 Ohm.m. It can be considered as a saturated zone with resistivity increase westward direction and their thickness varies from 14 to 36 m with increase south ward direction. The second zone (C2) exhibits relatively high resistivity than the above units (C1) with resistivity ranges from 21 to 40 Ohm.m that the increasing values towards the western side. The thickness of this unit (C2) exhibits values 20 m in the southern side and increasing towards the northwestern side to reach 40 m. The last saturated zone (C3) has higher resistivity values than the above another zone that range from 31 to 54 Ohm.m due to less clay content and coarse sand. This reflects good quality of groundwater downwards. The isopach contour map of this zone exhibits decreasing in its values (16-50 m) towards the northeastern directions.

The groundwater flow direction (Figure 15) is generally showing two directions; one toward north eastern and the other toward south western. This is probably due to the faulting effect detected in the aforementioned geoelectrical cross sections which impact on the water level. Figure 16 shows that the depth to water is increasing from east to west with a slight local increase toward northeast depending on the topography of the ground surface.

Hydrochemical facies and trends in groundwater composition

Chemical classification of subsurface waters from sedimentary basins aids in interpreting the complex processes involved in producing their dissolved solids, to better understand their origin and evolution. Water quality data may be interpreted on the basis of both individual analyses and sets of analyses from one sampling site or different sampling sites in an area or aquifer being examined. Collectively, water analyses may be compared and interpreted using areal plots, graphical methods, and statistical analyses. In this paper, both the areal plots (such as contour maps) and graphical methods (such as Chadha [32] and x-y scattered diagrams) will be used to detect the chemical trends and mixing of the different aquifers in the study area.

According to Chebotarev [33], groundwater samples have a fresh water type (TDS from 270 mg/l to 780 mg/l), except two samples (W9 and W12) showed brackish water type (TDS 1090 mg/l and 2600 mg/l). The pH values range from 6.9 to 8.2. Although the groundwater samples are few, they reflected a wide range of chemical water types. Theses water types are computed by Aquachem program. These water types were chosen on the basis that each ion that exceeds 22 epm% is included in water type

The ion contents of groundwater in the area are variable. This is probably due to the variety of recharging sources, ion

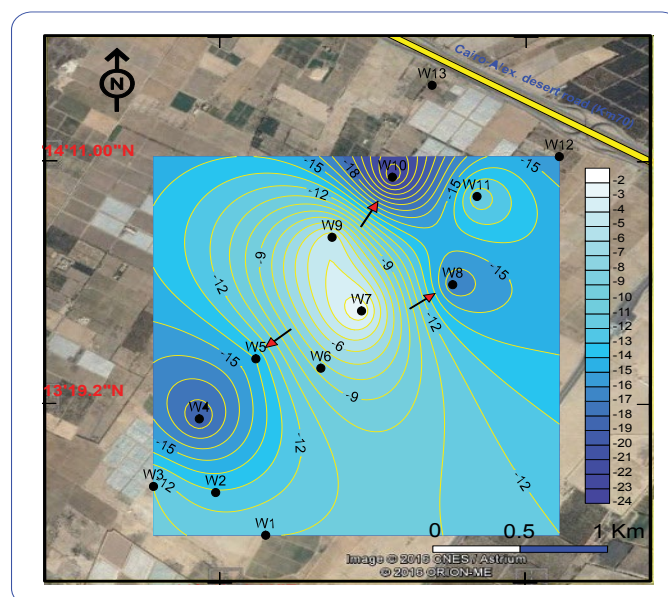


Figure 16: Depth to water contour map

exchange processes or mixing extents between Miocene and Oligocene groundwater. These hypotheses are assumed due to the appearance of different water types shown in Figure 13. These waters are mainly belonging to Na-Mg-Ca-HCO₃ and Na--Ca-Mg-HCO₃ (westward) intruded with chloride ion greater or smaller than bicarbonate. Locally, in the central part of the study area, Na-Cl-SO₄ water type was developed. The water of Na-Ca-Mg-Cl type evolves eastward close to Cairo-Alexandria desert road. This variable change in water type might be due to the effect of fluvial and fluvio-marine deposits and the lateral recharge from the Pleistocene aquifer [10] or due to the vertical seepage from the underlying Oligocene aquifer [34]. It is obvious that groundwater is changing evolutionary from HCO₃-Cl/Cl-HCO₃ type into Cl-SO₄, then to chloride type from west to east. Water salinity contour map showed that TDS increases all ways toward north, northeast and also shows a slight increase toward the south west (Figure 17). This compatible with the iso-resistivity contour maps (Figure 14) of the saturated geoelectrical layer (C) that represent low resistivity values due to an increase of clay content and showed also consistency with the groundwater flow direction (Figure 15).

Cross plots

The nature and the extent of water/rock interaction were assessed by plotting some relations between major ions. The Na-Cl relationship has often been used to identify the reasons of salinity in groundwater [35]. A Na⁺/Cl⁻ ratio equal to 1 is attributed to the dissolution of NaCl while a ratio greater than 1 reflects a release of Na⁺ from silicate weathering [36]. Refer to Na-Cl plot (Figure 18), almost all samples points around the 1:1 equiline suggesting that salt rocks dissolution and/or evaporation processes are favored. Ion exchange can be a source of sodium in the groundwater by releasing of Na from clay products. In order to confirm the ion-exchange process taking place, Na vs. Ca & Na vs. Mg relations are also plotted (Figures 19 and 20). In these two plots, the groundwater shown slightly elevated levels

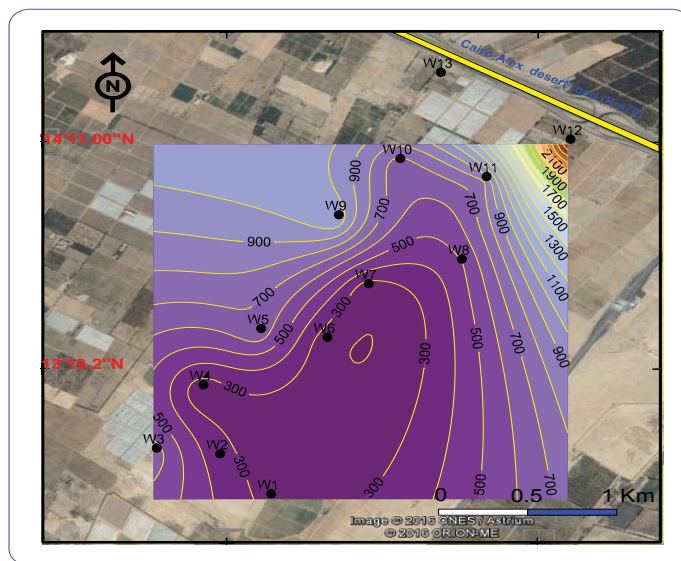


Figure 17: Iso-salinity contour map in the study area

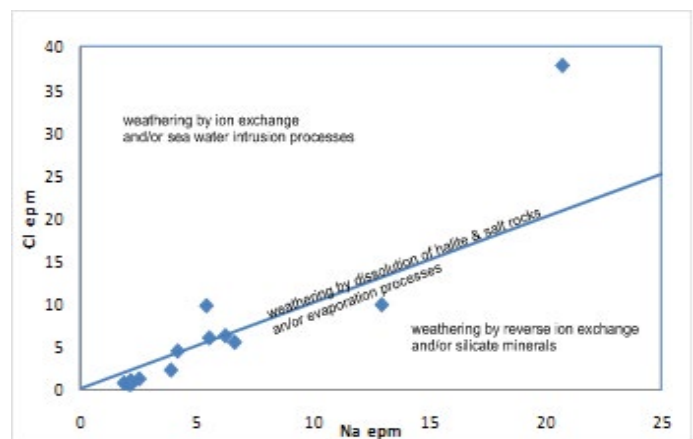


Figure 18: Na vs. Cl scatter diagram

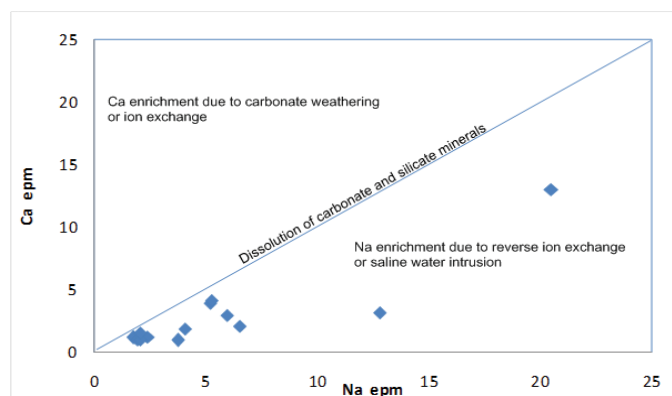


Figure 19: Na vs. Ca scatter diagram

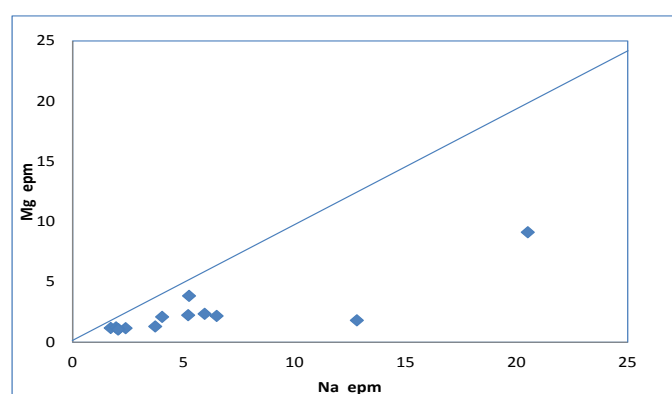


Figure 20: Na vs. Mg scatter diagram

of sodium compared to calcium and magnesium, implying the reverse ion exchange by adsorption of Ca & Mg ions and/or the release of Na to ground water. The Na vs. HCO_3^- (Figure 21) scatter diagram supports the same process and showing also few samples that point above the 1:1 equiline indicating calcite and/or clay minerals dissolution. Reverse ion exchange and dolomite dissolution are suggested by plotting the relations between Ca and Mg and between Cl and Mg/Ca in the groundwater samples (Figures 22 and 23).

Durov diagram is based on the percentage of the major ions in meq/L. Both the positive and the negative ion percentages total 100 %. In the Durov diagram, the cations specify the parameters of the left triangle and anions specify the parameters for the upper triangle. The cations and anions values are plotted on the appropriate triangular plots and the data points are projected onto the square of the main field. The advantage of this diagram over Piper's is that this diagram displays some possible geochemical processes that could affect the water genesis [37,38]. The fields and lines on the diagram show the classifications of Lloyd and Heathcoat [37].

The results of the analyzed samples were plotted on Durov diagram as presented in (Figure 24). According to the classification of Lloyd and Heathcoat [37], the groundwater in the study area reflect the prevailing of ion exchanges and reverse ion exchange of Na-Cl water due to the presence of some clay beds or lenses in the study area. Other diagenetic processes by dissolution; leaching and simple mixing affecting water quality (water points in field 5) may indicate the connection with other water bearings.

Chemical data of representative samples from the study area are also presented by plotting them on Chadha [32] diagram (modified piper' diagram, 1999) (Figure 25). These diagrams reveal the analogies, dissimilarities and different types of waters in the study area, which are identified by aquachem program (Figure 13). The distribution of samples on this plot shows that groundwater in the area under consideration is affected by different factors. These factors are; the lateral seepage from the adjacent quaternary aquifer, the vertical seepage from the underlying Oligocene aquifer and the leaching and dissolution processes. To delineate and identify the most important factor that affects groundwater quality, stable isotopes (O-18 & Deuterium) are considered in this discussion.

The isotopic compositions of oxygen-18 and deuterium in surface water and groundwater are very powerful tools for knowing the recharges sources to groundwater. Acquiring this characteristic is attributed to the relatively conservative

nature concerning the reaction with soil and aquifer materials. Otherwise, the isotopic composition ($\delta^{18}\text{O}$ and δD) of a water body remains as it is if this water does not subject to evaporation or mixing with other water that has a different isotopic composition [39].

To identify the possible recharging sources to the Miocene aquifer, the isotopic contents of the following relevant recharge resources (reference points) are considered for comparison:

- 1) The Pleistocene aquifer adjacent to the Miocene aquifer in the study area recorded as an average of 2.30‰ and 9.23‰ for $\delta^{18}\text{O}$ and δD , respectively) (samples 1, 2, 3 & 4 in El-Gamal [40]).
- 2) The Oligocene aquifer at the fringes of the Miocene aquifer in the study area recorded as (-3.06‰ and -26.50‰, for $\delta^{18}\text{O}$ and δD , respectively), (sample No. 24 in El-Gamal [40]).
- 3) Alexandria local rainwater ($\delta^{18}\text{O}=-4.6\%$ and $\delta\text{D}=-16.5\%$) (Hamza et al. [41]).
- 4) Al Nasr canal, representing the nearest branch of the Nile River close to the study area, ($\delta^{18}\text{O}=2.28\%$ and $\delta\text{D}=20.61\%$) (El Sayed et al. [42]).

The isotopic composition of these various resources and those of the collected groundwater samples are plotted as $\delta^{18}\text{O}$ - δD diagram (Figure 26). On the diagram, all groundwater samples collected from the study area are completely separated from the assumed relevant recharge sources except the Pleistocene sample and have higher positive $\delta^{18}\text{O}$ and δD values comparing with them. Although the area was subjected to local rainfall intensity (110 mm/year, averagely) and to the heavy rain storm event of 1994, the contribution from these rains to groundwater is ineffective. The isotopic compositions of these rains on the $\delta^{18}\text{O}$ - δD diagram are greatly different from those of the study groundwater and surface water samples. The mixing with the adjacent groundwater of the Pleistocene is confirmed. However mixing with the deeper aquifers needs more evidence. For this reason, Cl- O^{18} relationship is plotted (Figure 27). Refer to this plot, it is apparent that there are two groups; one of them is relatively depleted in its isotopic content, the other group is relatively enriched. Both of the two groups did not show correlative relationship reflecting the effects of dissolution of aquifer salts, besides the mixing with the deeper aquifer via over pumping or the fractures proved by geoelectrical measurements in this study. This conclusion is aided by contouring the values of O-18 (Figure 28). This figure separates groundwater sample into three zones which are somehow compatible with the aforementioned geoelectrical cross- section.

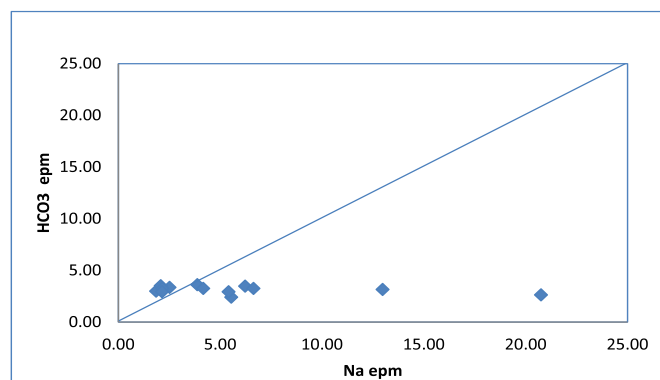


Figure 21: Na vs. HCO_3 scatter diagram

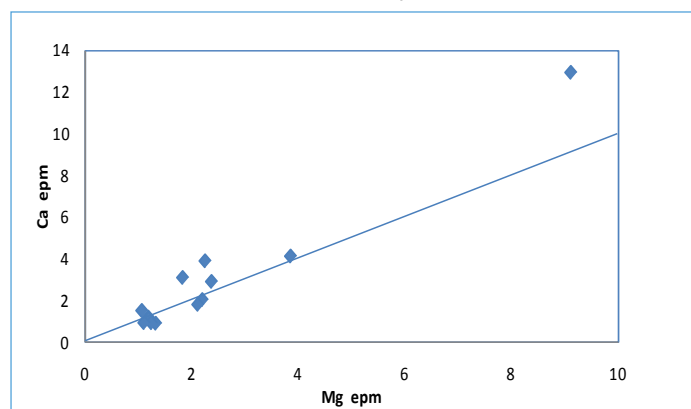


Figure 22: Mg vs. Ca scatter diagram

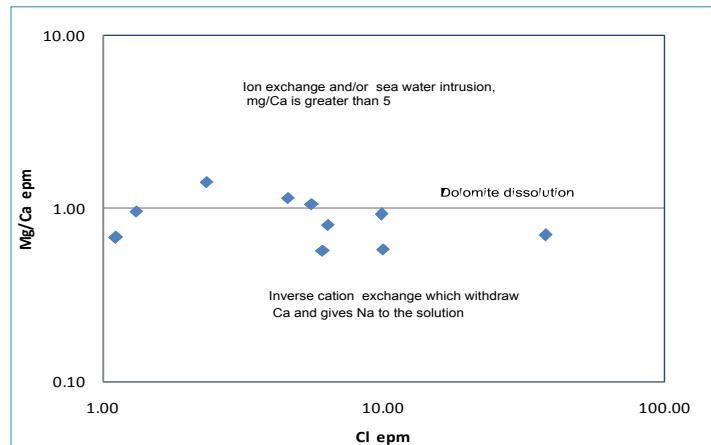


Figure 23: Cl vs. Mg/Ca scatter diagram

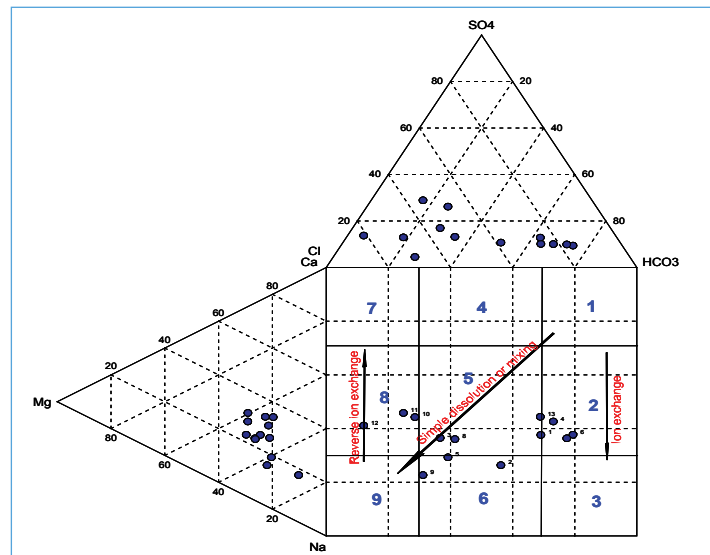


Figure 24: Durov diagram according to Lloyd and Heathcoat [37] classification

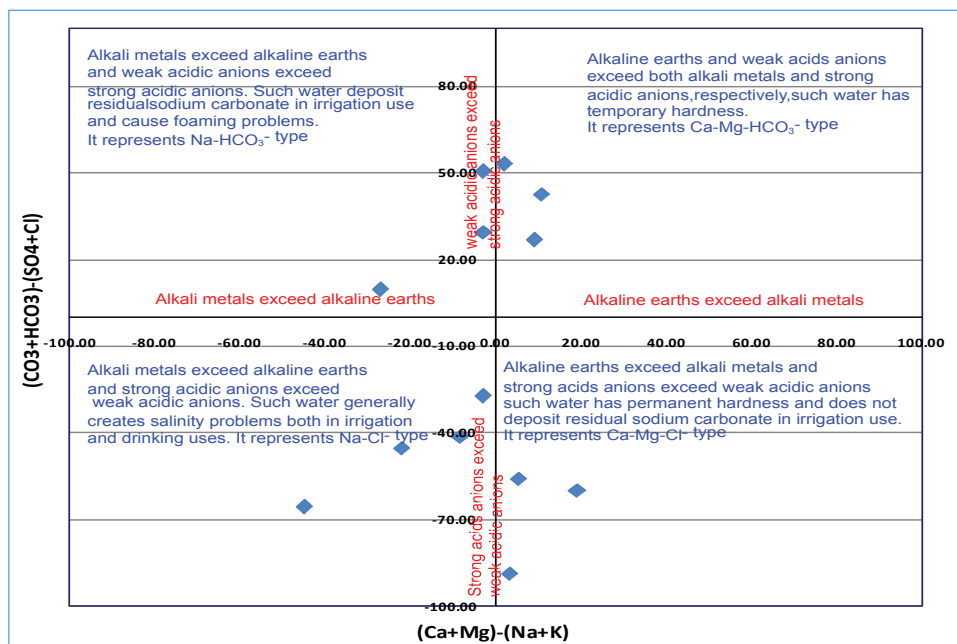


Figure 25: Modified piper's diagram Chadha [32]

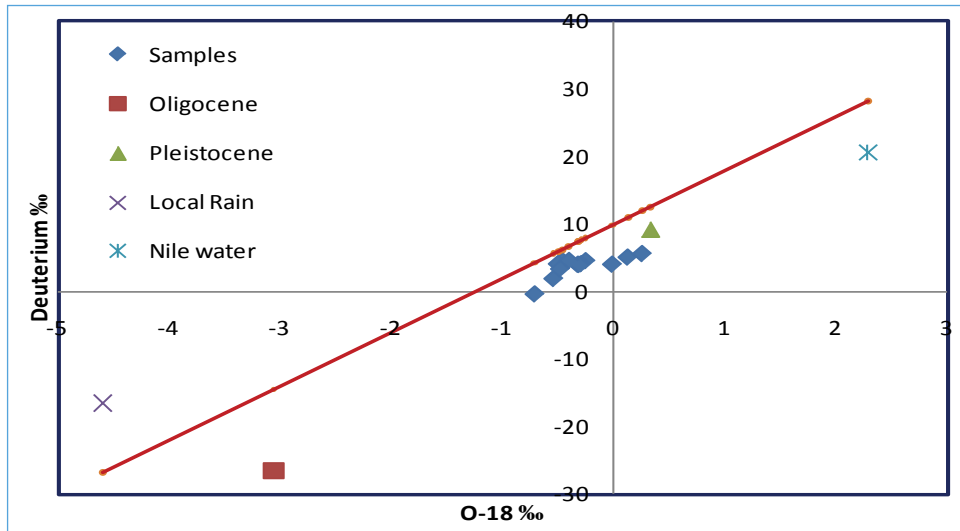


Figure 26: O-18 & deuterium relationship

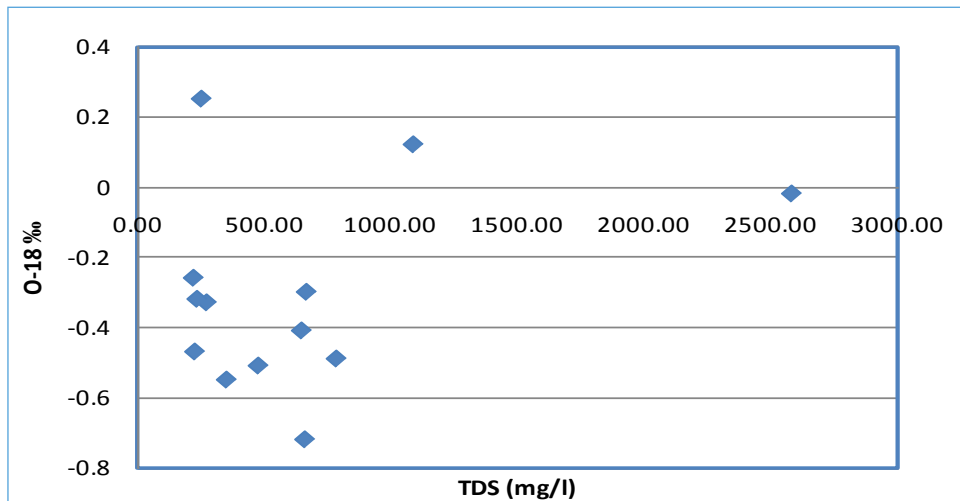


Figure 27: TDS vs. O-18

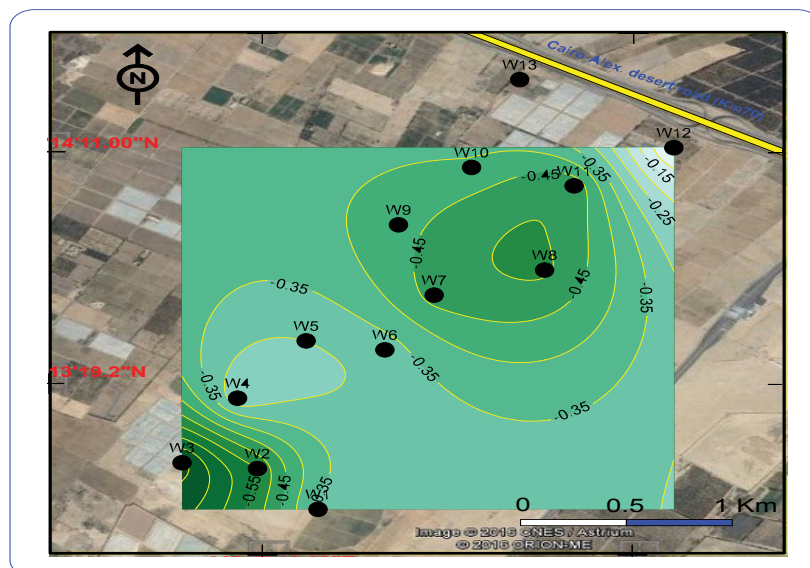


Figure 28: O-18 contour map

Layer No.	Resistivity (Ohm.m)	Thickness (m)	Corresponding Lithology	
A	15-507	2.2-4.6	Sand, gravel & clay	
B	20-117	91-102	Sand & clayey sand	
C	C1	15-26	14-38	clayey sand
	C2	21-40	20-40	Sand & clay
	C3	31-54	16-50	Coarse sand
D	>75	*****	Basalt	

Table 1: Resistivity, thickness ranges and the corresponding lithologic composition of the detected geoelectrical layers

CONCLUSION AND RECOMMENDATIONS

The present work applies an integration between geoelectrical survey and geochemical for groundwater potentiality in the area lies at 70 km from Cairo of Cairo-Alexandria desert highway. The study area is a part of the old alluvial plain which is characterized by a rolling surface sloping to the north and northeast. Many serious hydrogeological problems were concerning groundwater potentiality and degradation of quality. Several factors play a significant role in the occurrence and supply of groundwater such as sedimentary succession, the geologic structure, lateral facies change and bad managements like over pump and random drilled wells. The present study considered as a trial to deal with these groundwater conditions that effect on the sustainable development. The study area represents the alluvial plain covering the ground surface of the area. The subsurface of the area consists of sedimentary deposits belonging to Tertiary and Quaternary. These sediments consist mainly of gravel, sand, clay, clayey sand and sandy clay separated in the Oligocene time by the basaltic sheet. To achieve the aim of the study, a total of 12 Vertical Electrical Soundings (VES) in free wells and one 2D imaging with a roll along technique were carried out in the area of study. Also, the available data of 13 drilled wells were used that comprised lithological description, the thickness of the successive layers, water sample, and depth to water.

The interpretation results revealed that the subsurface sequence in the area under investigation from the top downwards, as "A", "B", "C" and "D" based on the geologic information. The third geoelectrical layer (C) corresponding to saturated layer and divided into three zones (C1, C2 & C3) according to resistivity values. The first zone (C1) composed from clayey sand with resistivity values ranging from 15 to 26 Ohm.m and their thickness varies from 14 38 m. The second zone has relatively high resistivity value due to less clay content with sand. The resistivity value of this zone ranging from 21 and 40 Ohm.m and thickness varies from 20 to 40 m. The last geoelectrical not extend all over the subsurface of the area due to faults with resistivity values ranging from 31 m to 54 Ohm.m. The high resistivity value is due to coarse sand but this zone end by clay content as well data. The thickness of this zone is ranging from 16 to 50 m. The result of the roll along two-dimensional resistivity imaging profile refers to the heterogeneous character of the upper surface due to different degrees of clay contents that increase north western side of the investigated area. The three detected zones reflect three geoelectrical layer with different thickness due to the effect of two faults (F1&F2) which throw northern trend detected that affect the subsurface succession.

According to the chemical and isotopic analysis data, groundwater in the area under consideration can be divided into two zones; fresh zone and brackish zone. The fresh zone is mainly recharged from the adjacent Pleistocene groundwater. The brackish zone is due to the vertical seepage from the underlying Oligocene groundwater via fractures or due to over pumping. The irregular lateral change in salinity could be also attributed to clay intercalations within the aquifer material.

Finally, the hydrogeological problems in the study area that cause an increase in salinity and draw down for water table due to the following and must be taken into consideration:

- Drilling of the new wells must be based on careful investigations.
- Random drilling wells and there is no safe distance between them.
- Over bump and no consider safe yield for every drilled well.
- The existing fault causes variation in the thickness of water bearing.

- The sediments of the water bearing not homogeneity and the clay content play an important role in the quality of groundwater.
- The design of drilled wells must be done on data logging.
- The Electric data logging for drilled well is very important.
- Follow new irrigation system and not allowing flood irrigation method to avoid water logging preamble.

The last water bearing layer is considerably the best one than above.

REFERENCES

- [1] Dawoud MA, Darwish MM, EL-Kady MM. GIS-based groundwater management model for western Nile Delta. *Water Resour Manag*, **2005**, 19: 585-604.
- [2] Pavlov MI. Groundwater of Egypt: Special report. Desert Institute, Cairo, Egypt, **1962**.
- [3] Saad K. Groundwater studies of Wadi El Natrun area and its vicinities. Desert Institute, Cairo, Egypt, **1962**.
- [4] Shata AA. The geology, origin and age of the groundwater supplies in some desert areas of U.A.R. Bull Inst du, Desert Egypt, **1962**, 12: 61-124.
- [5] Geoistrazivanja. Comprehensive technical report about test wells in the western desert fringes. Report Presented to Ministry of Public Works, **1962**.
- [6] La Moreaux PE. Reconnaissance report and recommendations for groundwater investigations. Wadi El Natrun, Western desert of Egypt report prepared for general desert development organization (G.D.D.O), Egypt, **1962**.
- [7] El Shazly EM, Abdel Hady MA, El Ghawaby MA, El Kassas IA, El Khawasik SM, et al. Geological interpretation of Landsat satellite images for west Nile Delta area, Egypt. Remote Sensing Research Project, Academy of Scientific Research and Technology, Egypt, **1975**.
- [8] Diab MSH, Abd el Latif AT, Abdel Baki AA. Groundwater occurrence in the southern sector of Cairo-Alexandria desert road. *Annals of Geological Survey of Egypt*, **1980**, 797-805.
- [9] RIGW and IWACO. Monitoring and control groundwater pollution in the Nile Delta and adjacent desert areas, El Kanater El Khairia, Egypt, **1991**.
- [10] Awad MA, Sallouma MK, Gomaa MA, Ezzeldin MR. Comparative hydro geochemical and isotopic studies on groundwater in Wadi El-Farigh and Wadi El-Natrun at the fringes of western Nile delta, Egypt, *El Minia Sci Bull*, **1997**.
- [11] Atwia MG, Hassan AA, Ibrahim ShA. Hydrogeology, log analysis and hydrochemistry of unconsolidated aquifers south of El-Sadat city, Egypt, *Hydrogeol J*, **1997**, 5: 27-38.
- [12] Dahab K, Sadek MA, El Fakharany MA. Replenishment and mineralization processes of lower Miocene aquifer at Wadi El Farigh area and its vicinities, using environmental isotopes and hydrochemistry. *Sci J Fac Sci*, **1999**, 111-127.
- [13] Awad SR. Impacts of developments activities of groundwater in the Nile Delta aquifer Egypt. Proceedings of the Round Table Meeting on Planning for Groundwater Development in Arid and Semi-Arid regions Cairo, Egypt, **2001**.
- [14] Atta SA. Pollution of shallow and groundwater in Delta region, Egypt. *Sci Bull Fac Eng*, **2002**, 37: 251-262.
- [15] Embaby AAA. Environmental evolution for the geomorphological situation in relation to the water and soil resources of the region north of the Sadat city, West Nile Delta, Egypt. Unpublished Ph.D. Thesis, Mansoura University, Faculty of Science, Egypt, **2003**.
- [16] Dawoud MA. Design of national groundwater quality monitoring network in Egypt. *Environ Monit Assess*, **2004**, 96: 99-118.
- [17] El Abd EA. The geological impact on the water bearing formations in the area southwest Nile Delta, Egypt. Unpublished Ph.D. Thesis, Menufiya University, Faculty of Science, Egypt, **2005**.
- [18] Youssef AMA. Impact of the subsurface structure on the groundwater occurrences in the southeastern part of wadi El Farigh, west of the Nile Delta, Egypt. *Desert Inst Bull*, **2000**, 50: 19-40.
- [19] Barseem MSM, El Sayed AN. Application of the geoelectrical method to study the factors affecting on the groundwater quality in the area to the west of Kilometer 117 along the Cairo-Alexandria Desert road, West Nile Delta (Case study). *Egypt J Desert Res*, **2008**, 58: 229-242.
- [20] El Sheikh AE, Ahmed KA. Study the impact of the basalt occurrence on the potentialities of groundwater aquifers in the southwestern delta area, Egypt for sustainable development. *Egypt J Geol*, **2016**, 60: 19-35.

-
- [21] Shata AA, El Fayoumy IF. Geomorphological and morphopedological aspects of the region west of the Nile Delta with special reference to Wadi El Natrun area. *Inst Desert d`Egypt*, **1967**, 1: 1-28.
- [22] Abd El Baki AA. Hydrogeological and hydro-geochemical studies on the area west of Rosetta branch and south El Nasr Canal. Ph.D. Thesis, Faculty of Science, Ain Shams University, Egypt, **1983**.
- [23] Abdel El-Rahman AA. Geophysical study on the groundwater conditions in the area southwest of the Nile Delta between Abu Roash and El-Khatatba road, Faculty of Science **1996**, Ain Shams University, Egypt.
- [24] Sandford KS, Arkell WG. Paleolithic man and the Nile valley in Lower Egypt. Chicago University, Oriental U.S.A. Inst Public, **1939**, 49: 105.
- [25] RIGW and IWACO. Vulnerability of groundwater to pollution in the Nile Valley and Delta, El Kanater El Khairia, Egypt, **1990**.
- [26] El Ghazawi MM. Geological studies of quaternary-neogene aquifer in the area northwest Nile Delta. Faculty of Science, Al-Azhar University, Cairo, Egypt, **1982**.
- [27] Abdel El-Rahman AA. Geoelectrical interpretation to solve the problem of salinization of the groundwater, East of Cairo-Alexandria Desert way at 80 km, Egypt (Case study). *Egypt J Appl Geophys*, **2012**, 11: 25-39.
- [28] El Fayoumy IF. Geology of groundwater supplies in wadi El Natrun area: M.Sc. Thesis, Faculty of Science, Cairo University, Egypt, **1964**.
- [29] Omara SM, Sand S. Rock stratigraphy and structural features of the area between Wadi El Natrun and Moghra depression, western desert, Egypt, *Geol Jb Bl*, **1975**, 6: 45-73.
- [30] El- Sayed SA. Hydrogeological and isotope assessment of groundwater in wadi El Natrun and Sadat City, Egypt, Ain Shams University, Cairo, Egypt, **1999**, 237.
- [31] Dahlin T, Loke MH. Resolution of 2D Wenner resistivity imaging as assessed by numerical modeling. *J Appl Geophys*, **1998**, 38: 237-249.
- [32] Chadha K. A proposed new diagram for geochemical classification of natural water and interpretation of chemical data. *Hydrogeology J*, **1999**, 7: 431.
- [33] Chebotarev IL. Metamorphism of natural waters in the crust of weathering. *Geochem Acta*, **1955**, 8: 23-48.
- [34] El Ghazawi MM, SM Atwa. Contributions of some structural elements to the groundwater conditions in the southwestern portion of the Nile Delta. Geological Society of Egypt, Cairo, Egypt, **1994**, 38: 649-667.
- [35] Banton O, L Bangoy. Hydrogeology: The groundwater environmental multi science. Presses del' Université du Québec, Sainte-Foy, Quebec, **1997**, 460.
- [36] Meybeck M. Global chemical weathering of surficial rocks estimated from river dissolved loads. *Am J Sci*, **1987**, 287: 401-428.
- [37] Lloyd JW, Heathcoat JA. Natural inorganic chemistry in relation to ground water. Clarendon Press, Oxford, **1985**.
- [38] Ziad Q. A hydrogeological, hydrochemical and environmental study in Wadi Al Arroub drainage basin, south west Bank, Palestine. Institut fur Geologie/LHS Hydrogeologie, TU Bergakademie Freiberg, **2003**.
- [39] Kendall C, Sklash MG, Bullen TD. Isotope tracers of water and solute sources in catchments. John Wiley & Sons Ltd, USA, California, **1995**, 261-303.
- [40] El-Gamal H. Environmental tracers in groundwater as tools to study hydrological questions in arid regions. Combined Faculties of the Natural Sciences and for Mathematics of the Ruperto-Carola University of Heidelberg, Germany, **2005**.
- [41] Hamza MS, El-Malky MG, Sadek MA, Taher A, Rayan RA et al. Using environmental isotopes and hydrogeochemistry for determining factors of rising water table below Greco-Roman Antiques localities in Alexandria city, Egypt. *J Environ Sci*, **2009**.
- [42] El-Sayed SA, Atta ER, Al-Ashri KM. Ground water table rise in northwest Nile Delta: Problems and recommendations. *J Rad Res Appl Sci*, **2012**, 5: 141-171.